

Collapse of a single polymer chain: Effects of chain stiffness and attraction range

Yanyan Zhu,^{1,2} Haim Diamant,^{2,3,*} and David Andelman^{1,2,†}

¹*School of Physics and Astronomy, Tel Aviv University, Ramat Aviv 69978, Tel Aviv, Israel*

²*Center for Physics and Chemistry of Living Systems, Tel Aviv University, Tel Aviv 69978, Israel*

³*School of Chemistry, Tel Aviv University, Ramat Aviv 69978, Tel Aviv, Israel*

ABSTRACT

Chain-like macromolecules in solution, whether biological or synthetic, transform from an extended conformation to a compact one when temperature or other system parameters change. This collapse transition is relevant in various phenomena, including DNA condensation, protein folding, and the behavior of polymers in solution. We investigate the interplay of chain stiffness and range of attraction between monomers in the collapse of a single polymer chain. We use Monte Carlo simulations based on the pruned-enriched Rosenbluth method. Two distinct behaviors are found depending on chain stiffness (represented by the persistence length l_p) and attraction range r_c . When l_p is larger than r_c , the chain collapses sharply with decreasing temperature, whereas if l_p is smaller than r_c , it contracts gradually. Notably, in the regime of small l_p and large r_c , this rounding into a gradual compaction persists upon increasing the chain length and may remain in place in the limit of infinite chain length. Furthermore, for small r_c , the transition temperature (θ -temperature) increases with l_p , whereas for large r_c the θ -temperature decreases with l_p . Thus, stiffness promotes collapse for small r_c but suppresses it for large r_c . Our findings are in agreement with recent experiments on the contraction of single-stranded RNA as compared to double-stranded DNA, and provide valuable insights for understanding polymer collapse and the essential polymer parameters affecting it.

I. INTRODUCTION

Single-chain collapse refers to the conformational transition of a polymer chain from an extended coil-like structure to a compact globular state in response to external changes such as temperature or pH [1–4]. This thoroughly studied phenomenon is fundamental in polymer science and related to the commonly observed processes in biomacromolecules, *e.g.*, protein folding and denaturation, as well as in synthetic polymers [5–7].

The coil-to-globule transition was first predicted by Stockmayer in 1960 [8] and later observed experimentally by Tanaka and co-workers [9, 10]. Over the past half-century, extensive research, encompassing both theoretical and experimental studies, has been conducted to investigate the collapse of single chains. Lifshitz [11] and later Lifshitz, Grosberg, and Khokhlov [12] pioneered the theoretical framework for the coil-to-globule transition in homopolymers, which was later refined by Grosberg and co-workers [13]. Subsequently, it was validated through experiments on synthetic macromolecules [14, 15] using various experimental techniques, including light scattering and viscometry [16–19].

While many uncharged synthetic polymers are flexible, polyelectrolytes and important biopolymers, such as DNA, bio-filaments, and certain proteins, exhibit semi-flexibility due to chain stiffness [20, 21]. This behavior

is characterized by a persistence length l_p , which is the characteristic distance over which the chain maintains its direction. The distinction between flexible and semiflexible chains is very relevant to the chain collapse, and a large body of research [22, 23] has focused on how the stiffness of semiflexible polymers affects their phase behavior, including the formation of different condensates such as rod-like and toroidal structures [24–28].

Theoretical studies have shown that the nature of the single-chain collapse transition depends sensitively on chain stiffness. For flexible polymers, the collapse corresponds to the θ -transition, which is continuous (second-order) in the thermodynamic limit [29, 30]. In contrast, for semiflexible or sufficiently stiff polymers, the transition can become discontinuous (first-order), reflecting a qualitatively different collapse mechanism [1, 31–33].

Regarding the effect of chain stiffness on the transition temperature T_θ , the natural expectation is that increased stiffness should hinder compaction, leading to *lower* T_θ . Indeed, this trend was observed in many simulations [26–28]. However, an early mean-field theory by Doniach, Garel, and Orland [34] predicted that T_θ should be *independent* of stiffness. Yet, a later work by Bastolla and Grassberger [35] suggested that T_θ should *increase* with stiffness. These different results indicate that the effect of chain stiffness on T_θ remains an intricate open question.

Much less work has been devoted to the effect of the range of monomer-monomer attraction on the collapse transition. In a series of Monte Carlo simulations, Binder, Paul, and co-workers [36–38] investigated the phase diagram of a single polymer chain as a function of temperature and the range of a square-well attrac-

* hdiamant@tauex.tau.ac.il

† andelman@tauex.tau.ac.il

tive interaction. Their results demonstrated that altering the interaction range could lead to a collapse transition into different conformational states, including a collapsed globule and a compact crystallite.

The renewed interest in these fundamental single-chain issues has been recently motivated by experiments by Knobler, Gelbart, and their co-workers [39], who investigated the condensation of long double-stranded DNA (dsDNA), as compared to long single-stranded RNA (ssRNA), in the presence of polyvalent cations. While the dsDNA undergoes discontinuous condensation at a critical ion concentration, the ssRNA exhibits gradual compaction over a wide concentration range. The large difference in stiffness between dsDNA and ssRNA probably underlies their distinct condensation behaviors. Thus, a general understanding of single-chain collapse scenarios would be valuable for tailoring polymer properties across diverse applications.

Motivated mainly by these recent findings [39], we revisit the single-chain collapse by focusing on the interplay between chain stiffness (l_p) and the range of intra-chain attraction (r_c), which is found to determine the sharpness and temperature of chain compaction. This interplay is accounted for in a way that was not systematically explored before. Our approach reveals how the attraction range and persistence length critically affect the polymer collapse. In particular, for small l_p and large r_c , the chain undergoes a smooth crossover where it continuously shrinks, rather than exhibiting a critical collapse transition. As we show below, this rounding does not disappear upon increasing the chain length.

This paper is organized as follows. Section II describes the model and simulation method. Section III presents our results and discussion, focusing on the transition sharpness and dependence of transition temperature on polymer stiffness, attraction range, and chain length. Section IV concludes with a summary of the findings and their experimental implications. Finally, the Appendix presents a heuristic scaling argument [40] for the rounding of the collapse transition due to the interplay between chain stiffness and condensing agents.

II. MODEL

A. The pruned-enriched Rosenbluth method

We model a polymer chain as a self-avoiding random walk (SAW) in three dimensions (3D) on a simple cubic lattice. Each monomer occupies one lattice site, and two monomers cannot occupy the same site, mimicking self-avoidance. To investigate the collapse of a single chain, we employed the Pruned-Enriched Rosenbluth Method (PERM) [41], which is an efficient Monte-Carlo (MC) algorithm to investigate single-chain collapse, as is explained next. It is based on the Rosenbluth-Rosenbluth (RR) pioneering MC algorithm [42], as well as on enrichment techniques, in which sample attrition is reduced by

replicating successful chains [43].

The chain configurations are built iteratively. At each step, the RR method adds a new monomer to the partially built chain. This n -th monomer occupies one of the $m_n \leq 5$ non-occupied neighboring sites on the 3D cubic lattice. The normalized probability p_k of selecting a specific site $k = 1, \dots, m_n$ for the n -th monomer is based on a Boltzmann weight in the following way:

$$p_k = e^{-\beta E_k} / \sum_{l=1}^{m_n} e^{-\beta E_l}, \quad (1)$$

where E_k is the energy associated with the k position and depends on the interaction with all nearby monomers, and $\beta = 1/k_B T$ is the inverse thermal energy. As the Boltzmann factor is included in the probability p_k , the corrected weight w_n associated with the k position, is *independent* of k

$$w_n = e^{-\beta E_k} / p_k = \sum_{l=1}^{m_n} e^{-\beta E_l}, \quad (2)$$

and reflects the principle of ‘importance sampling’, where the Boltzmann bias in p_k is compensated by the weight factor w_n (see Ref. [41] for more details).

The total weight W_N of a specific chain configuration composed of N monomers is given by

$$W_N = \prod_{n=1}^N w_n. \quad (3)$$

The RR method for simulating statistics of long chains is known to fail for long polymer chains due to two main reasons [41, 44]. The first is the ‘attrition problem’, where steps with no valid placement cause most attempts to terminate, and consequently, only a small fraction of chains reach the full length, especially for large N . The second is due to large fluctuations in the total W_N weight. The fluctuations in each of the w_n factors lead roughly to a log-normal distribution for W_N [41], Eq. (3). It results in having too large weights for some chain configurations, while other configurations have too small weights. Consequently, the surviving chain configurations are dominated by a single configuration, causing a substantial lack of sampling.

The *Pruned-Enriched* Rosenbluth Method (PERM) was developed to address these issues [41]. The key idea behind PERM is that, as the chain is grown, low-probability configurations are pruned, while high-probability ones are enriched, depending on their W_N weight. Two thresholds, W_N^+ and W_N^- , are introduced, defining ‘high’ and ‘low’ weights, respectively. In his original work [41], Grassberger set the ratio of the enrichment and pruning thresholds to be approximately 10. Such a choice of the ratio primarily affects the efficiency of PERM, but does not influence the simulation results themselves.

The PERM simulations are then conducted in the following way. For $W_N > W_N^+$, the configuration is enriched by duplication, so that two independent copies are propagated at the next growth step. Each copy is assigned half the weight of its ‘parent’, thereby ensuring that the total statistical weight is conserved. Conversely, for $W_N < W_N^-$, the chosen configuration is conditionally ‘pruned’ at the next step in the following way. We choose a uniformly distributed random number $x \in [0, 1]$. If $x < 1/2$, the configuration is discarded (pruned). Otherwise, it is retained, and its weight is multiplied by a factor of two, in order to preserve the total statistical weight.

B. The attraction and bending energy

In our model, monomers occupy distinct lattice sites, accounting for the excluded-volume repulsion. Therefore, the polymer chains represent a self-avoiding walk (SAW) on a 3D lattice. The energy E_k in Eq. (2) is taken as a sum of two terms,

$$E_k = u_{\text{att}}(r) + u_{\text{bend}}(\theta), \quad (4)$$

where $u_{\text{att}}(r)$ is the attractive energy between all pairs of monomers separated by a distance r in 3D space, and $u_{\text{bend}}(\theta)$ is the bending energy between two adjacent bonds of relative angle θ .

The attractive interaction, u_{att} , is required to obtain the chain collapse transition. As the form of this attraction does not matter substantially, we have used a simple form,

$$u_{\text{att}}(r) = \begin{cases} -\varepsilon \left(\frac{b}{r}\right), & r \leq r_c \\ 0, & r > r_c. \end{cases} \quad (5)$$

Here, r_c is a cutoff distance defining the range of attraction, ε characterizes the attraction strength, and b is the bond length.

The bending-energy term is given by

$$u_{\text{bend}}(\theta) = \frac{\kappa}{b} (1 - \cos \theta), \quad (6)$$

where κ is the bending stiffness, implying that the persistence length is $l_p = \beta\kappa$. In our model, the angle θ can only take the discrete values $0, \pm\pi/2$ (having different weights), associated with the 3D cubic lattice forward and sideways directions, while moving backward is not allowed for a SAW.

By substituting the expressions for u_{att} and u_{bend} , Eqs. (5) and (6), into Eqs. (2) and (4), we obtain the weight w_n of the n -th monomer,

$$w_n = \sum_{l=1}^{m_n} \exp \left[\frac{\beta\varepsilon b}{r_l} - \frac{l_p(1 - \cos \theta_l)}{b} \right]. \quad (7)$$

Here r_l is the position of the l -th candidate of the n -monomer, and θ_l is the angle between the trial bond direction and the previous bond.

In the analysis below, we choose $l_p = \beta\kappa$ rather than κ as the control parameter. As a result, only the attraction term in the exponential depends on temperature. Hereafter, we will use the rescaled (dimensionless) temperature $T^* \equiv k_B T / \varepsilon = 1/(\beta\varepsilon)$.

III. RESULTS AND DISCUSSION

A. Transition sharpness: Effect of l_p and r_c

We first conduct numerical simulations of polymer chains having a length of $N = 500$, with all lengths expressed in units of the bond length b . A total of approximately 10^5 chains were generated using the PERM algorithm. Averages of the gyration radius squared, $\langle R_g^2 \rangle$, are computed over the ensemble of successful polymer configurations. As the temperature decreases, the chain collapses as expected. We systematically investigate the influence of chain stiffness l_p and attraction range r_c on this chain collapse.

Figure 1a shows the dependence of the swelling factor of the gyration radius, $\langle R_g^2 \rangle / N$, on the reduced temperature, $T^* \equiv k_B T / \varepsilon$, plotted on a semi-log plot. The quantity $\langle R_g^2 \rangle / N$ serves as a measure of the chain average conformation, as will be further discussed in Sec. III B. Lines of the same color (blue, red, green) represent chains with the same attraction range r_c , while the same symbols (circle, square, triangle, diamond) correspond to chains with the same persistence length l_p .

As seen in Fig. 1a, the transition changes from gradual to sharp as the persistence length l_p increases. This trend is observed for chains with $r_c = 1$ (blue), $r_c = 2$ (red), and $r_c = 3$ (green). Conversely, for chains with the same persistence length l_p (denoted by the same symbol), the transition tends to become sharper as r_c decreases. The transition temperature exhibits different trends with increasing l_p , depending on r_c , as is further discussed in Sec. III B.

The sharpness of the transition clearly depends on the values of l_p and r_c . To quantify these differences, we fit in Fig. 1a the swelling factor data as a function of temperature to a sigmoid-like function,

$$\langle R_g^2 \rangle / N = A + B \tanh [C \ln(T^* / T_0)], \quad (8)$$

where A , B , C , and T_0 are fit parameters. Next, we calculate the derivative $d(\langle R_g^2 \rangle / N) / dT^*$ (i.e. slope) of each fitted curve, as shown in Fig. 1b and 1c. The maximum slope for each chain type, characterized by its l_p and r_c is indicated by symbols on each curve. For $l_p = 3$ (diamond symbols in Fig. 1a), although the global fit is less accurate, the location of the derivative peak remains robust. Figure 1b corresponds to $l_p = 3$, while Fig. 1c shows results for $l_p = 0, 1, 2$. For $r_c = 1$ in Fig. 1c (blue curves), deviations from an ideal sigmoid occur at low T^* due to the limited data range, but the derivative peak remains well defined.

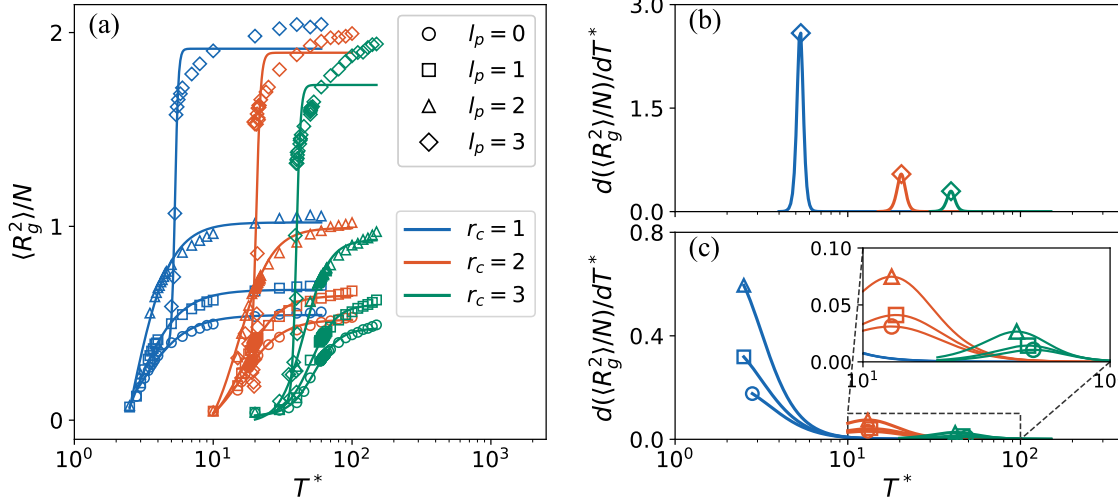


FIG. 1. (a) Swelling factor $\langle R_g^2 \rangle/N$ of the gyration radius as a function of rescaled temperature $T^* \equiv k_B T/\varepsilon$, plotted on a semi-log plot. Different symbols correspond to different values of the persistence length: $l_p = 0$ (circle), 1 (square), 2 (triangle), and 3 (diamond), while different colors denote different values of the attraction range: $r_c = 1$ (blue), 2 (red), and 3 (green). The curves are fits to a sigmoid-like function [Eq. (8)]. For $l_p = 3$, the fit is less accurate but the derivative peak remains reliable. (b) and (c) Derivative $d(\langle R_g^2 \rangle/N)/dT^*$ of the fitted curve as a function of the rescaled temperature T^* on a semi-logarithmic scale, for different values of l_p and r_c (legend in (a)). (b) $l_p = 3$; (c) $l_p = 0, 1, 2$. The inset in (c) shows an enlarged view of the $r_c = 2$ and 3 curves over a narrow range of small derivative values, highlighting the very weak peaks. The data correspond to chains with $N = 500$, and the bond length b is taken as the unit length.

It is evident that the maximum slope decreases with r_c and increases with l_p . For small l_p and large r_c (see the inset of Fig. 1c), the derivative $d(\langle R_g^2 \rangle/N)/dT^*$ becomes very small, indicating that the sharp transition is effectively removed. This behavior arises because a larger r_c leads to contraction of the entire polymer chain, thereby smoothing the transition and resulting in a more gradual compaction. The description of gradual contraction due to longer-ranged attraction is supported by a scaling argument, focusing on the case of chain collapse due to condensing agents, where r_c is determined by the correlation length among the condensing agents [40, 45] (see Appendix).

For the stiffest chains in our study, $l_p = 3$, we observe a sharp transition and significant fluctuations as the temperature passes through the transition. To further demonstrate the collapse behavior, we replot in Fig. 2a the data of Fig. 1a for $\langle R_g^2 \rangle/N$ as a function of T^* for the largest $l_p = 3$ and $r_c = 1, 2$, and 3. For $r_c = 2$, the inset of Fig. 2a shows the enlarged transition region in the temperature range $19 \leq T^* \leq 22$. Pronounced fluctuations in chain size are evident near the transition temperature, indicating a highly unstable polymer state.

In Fig. 2b, we plot the entire probability distribution $P(R_g)$ for different T^* values, where $l_p = 3$ and $r_c = 2$. As the rescaled temperature $T^* = k_B T/\varepsilon$ decreases from 21 to 18, the mean R_g initially decreases; yet, notably, at $T^* = 19$, a bimodal distribution emerges (blue histogram), indicating the coexistence of two dis-

tinct phases. This observation suggests that the collapse transition for stiff chains is first-order. Our results are consistent with earlier PERM simulations by Grassberger [35], who showed that sufficiently large stiffness leads to a first-order coil-folded transition.

For comparison, Fig. 2c and 2d show the corresponding results for smaller persistence lengths ($l_p = 0, 1$, and 2). In Fig. 2c, the swelling factor $\langle R_g^2 \rangle/N$ varies more smoothly with temperature, and the transition becomes progressively more gradual as l_p decreases. Consistently, the probability distributions in Fig. 2d exhibit a single broad peak that shifts continuously with temperature, indicating a gradual compaction of the chain. These observations are consistent with the experimentally observed discontinuous condensation of double-stranded DNA and continuous compaction of single-stranded RNA, supporting the relevance of our model to semiflexible polymer systems (e.g., Ref. [39]).

B. Transition temperature: Effect of l_p and r_c

For $N \gg 1$, $\langle R_g^2 \rangle$ scales with chain length as $\langle R_g^2 \rangle \sim N^{2\nu}$, where ν is the Flory exponent. Consequently, $\langle R_g^2 \rangle/N \sim N^{2\nu-1}$. This quantity provides a sensitive probe of the chain conformation. For $T > T_\theta$, the chain is swollen, and $\langle R_g^2 \rangle/N$ increases monotonously with N ($\nu > 1/2$). Whereas for $T < T_\theta$, $\langle R_g^2 \rangle/N$ initially increases with N and then, for large enough N , it de-

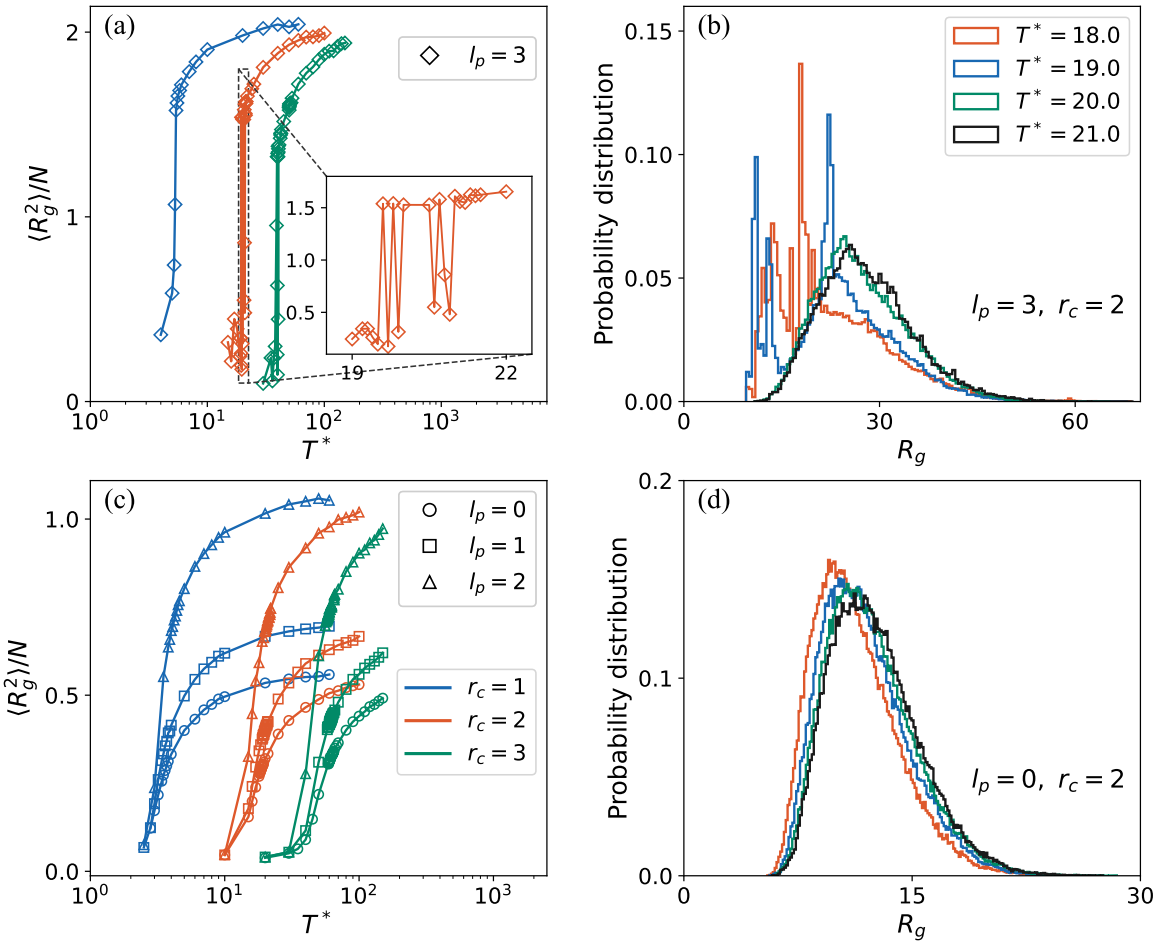


FIG. 2. (a) and (c) Swelling factor $\langle R_g^2 \rangle / N$ as a function of the rescaled temperature T^* on a semi-log plot. (a) for $l_p = 3$, and (c) for $l_p = 0, 1, 2$. The three colors correspond to different r_c values, as in Fig. 1 (see also the legend). Lines are guides to the eye. The inset in (a) shows an enlarged view of the $r_c = 2$ curve in the temperature range $19 \leq T^* \leq 22$. (b) and (d) Probability distribution histograms of R_g for different temperatures: $T^* = 18.0$ (red), $T^* = 19.0$ (blue), $T^* = 20.0$ (green), and $T^* = 21.0$ (black). For all temperatures in (b) $l_p = 3$ and $r_c = 2$, and in (d) $l_p = 0$ and $r_c = 2$. Only the histogram outline is shown for clarity. Results are for chains of length $N = 500$, and the bond length b is taken as the unit length.

creases, indicating an asymptotic value of $\nu < 1/2$. At $T = T_\theta$, $\nu \rightarrow 1/2$ for $N \gg 1$, and $\langle R_g^2 \rangle / N$ becomes approximately independent of N . Therefore, we identify the temperature closest to T_θ as the temperature where $\langle R_g^2 \rangle / N$ initially increases with N and then flattens out.

In Fig. 3, the swelling factor $\langle R_g^2 \rangle / N$ is plotted as a function of N on a semi-log plot for different temperatures, while keeping l_p and r_c fixed. Applying the above criterion, we identified the temperature at which the curve flattens out (the slope approaches zero) for large N as the closest to T_θ . However, near the transition temperature, the curves for different temperatures become similar, making visual determination difficult. Therefore,

our criterion to identify T_θ^* is to choose the curve having an almost zero slope (taken here to be less than 0.01). More specifically, in Fig. 3a, the slopes for $l_p = 0$ and $r_c = 2$, at large N and for $T^* = 18.8, 18.9$, and 19.0 (blue, green, and orange lines, respectively) are all below 0.01, indicating that $T_\theta^* \simeq 18.9 \pm 0.1$.

For stiffer chains, an illustrative example is shown in Fig. 3b for $l_p = 3$ and $r_c = 2$. Unlike the gradual collapse as a function of temperature, observed for flexible chains (Fig. 3a), the stiffer chains exhibit a markedly different behavior due to a first-order abrupt transition. This is seen in the temperature range, $20.6 \leq T^* \leq 20.9$, where the slope of $\langle R_g^2 \rangle / N$ as a function of N on a semi-log

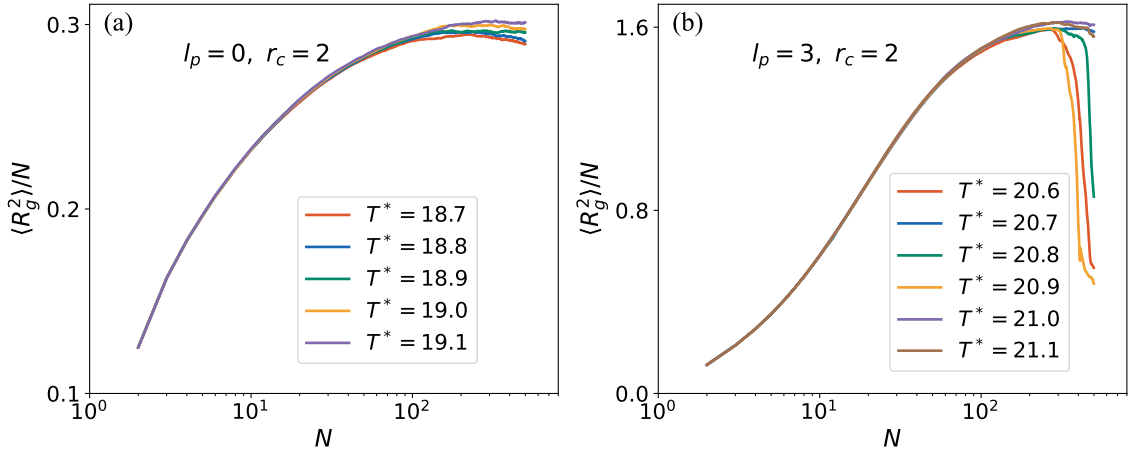


FIG. 3. Swelling factor, $\langle R_g^2 \rangle / N$, as a function of chain length, N , plotted on a semi-log plot. (a) $l_p = 0, r_c = 2$ for $T^* \equiv k_B T / \varepsilon = 18.7, 18.8, 18.9, 19.0$, and 19.1 (see legend). The transition temperature is estimated as $T^* \simeq 18.9 \pm 0.1$. (b) $l_p = 3, r_c = 2$ for $T^* = 20.6, 20.7, 20.8, 20.9, 21.0$, and 21.1 (see legend). The transition temperature is estimated as $T^* \simeq 21.0 \pm 0.1$.

plot shows a pronounced drop at large N . However, T_θ^* is determined as in Fig. 3a, as the temperature with the slope closest to zero, yielding $T_\theta^* \simeq 21.0 \pm 0.1$ (purple line).

l_p (blue curve), while for large r_c , T_θ^* decreases with l_p (green curve).

Thus, in addition to influencing the transition sharpness, the interplay between l_p and r_c also affects the behavior of T_θ . As mentioned in Sec. I, there have been conflicting reports in the literature [26–28, 34, 35] as to whether T_θ increases, decreases, or remains unchanged, with increasing stiffness. Our results and analysis suggest that *all three scenarios* are possible. As can be seen in Fig. 4, we find that for small r_c , T_θ increases with l_p , while for large r_c , it decreases with l_p . Namely, the manner in which stiffness changes T_θ depends qualitatively on r_c , the range of the attractive pair-potential between monomers.

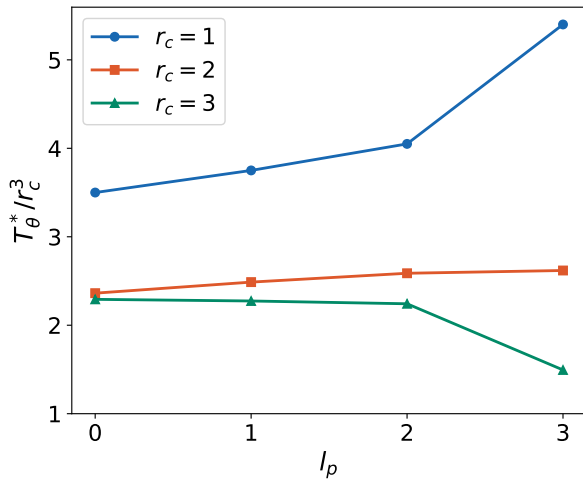


FIG. 4. Dependence of T_θ^* / r_c^3 on l_p for $r_c = 1, 2$, and 3 . All error bars are smaller than the symbol size. The chain length in all cases is $N = 500$, and the bond length b is taken as the unit length.

It is instructive to look at the transition temperature divided by r_c^3 , the volume of the attractive interaction range. A larger r_c means that more monomers are included within the interaction range, therefore shifting T_θ^* to higher values. Looking at T_θ^* / r_c^3 allows for a meaningful comparison across different r_c values and enables all T_θ^* values to be presented on the same plot. Figure 4 shows the dependence of T_θ^* / r_c^3 on l_p , for three values of r_c . For small r_c , T_θ^* increases with the persistence length

These different trends can be explained as follows. When r_c is small, increasing l_p favors the formation of hairpin structures, where a stiff chain can fold back on itself, creating many contacts. Figure 5 shows two typical chain configurations obtained from the simulations, one at $T_\theta^* = 5.4$ for $l_p = 3$ and $r_c = 1$, and the other at $T_\theta^* = 40.3$ for $l_p = 3$ and $r_c = 3$. A “typical configuration” refers to chains whose R_g is closest to the peak of the R_g distribution. Note that hairpins appear for $r_c = 1$ (Fig. 5a), but not for $r_c = 3$ (Fig. 5b). A hairpin is identified when two non-adjacent segments, separated by a contour distance s , are arranged in an anti-parallel fashion and remain spatially close over a finite segment of the contour. Once hairpins form, they promote chain collapse [35]. Consequently, for small r_c (e.g., $r_c = 1$), T_θ increases with increasing l_p . However, when the attraction range r_c is large (e.g., $r_c = 3$), increasing l_p just makes the chain more resistant to bending and contraction, and T_θ decreases with stiffness.

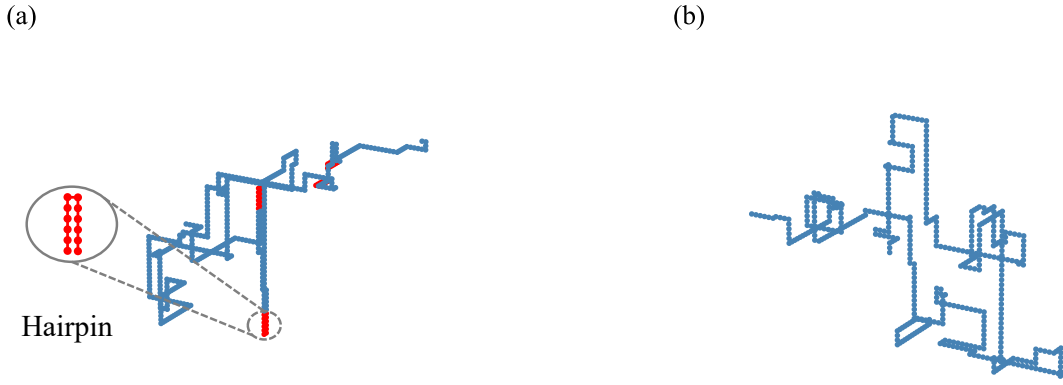


FIG. 5. (a) A typical chain configuration for $l_p = 3$ and $r_c = 1$ at $T_\theta^* = 5.4$, with the detected hairpin segment highlighted in red. A blow-up of the hairpin segment is also shown. (b) A typical chain configuration for $l_p = 3$ and $r_c = 3$ at $T_\theta^* = 40.3$ with no hairpins. In both cases, the chain length is $N = 500$.

C. Effect of chain length

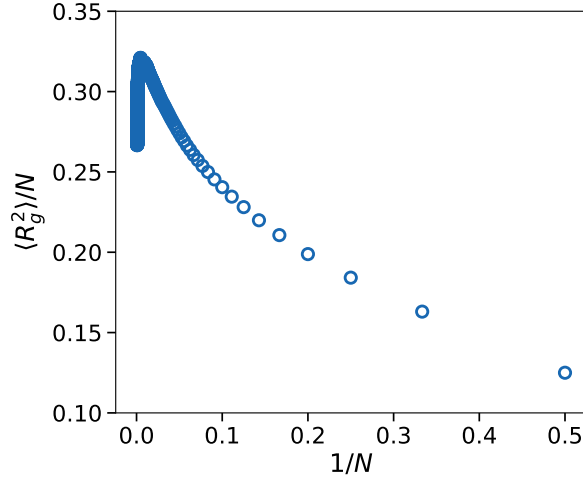


FIG. 6. Swelling factor $\langle R_g^2 \rangle / N$ as a function of $1/N$ at fixed temperature $T^* = k_B T/\epsilon = 60$, for polymer chains of length up to $N = 1,500$, in the case $l_p = 0$ and $r_c = 3$.

Having shown how l_p and r_c influence the collapse transition, we now examine the chain length's role on the transition temperature and sharpness. The main motivation is to analyze the behavior for exceedingly long chains. In the preceding sections, we fixed the chain length at $N = 500$. However, to examine the finite-size effect, we vary the chain length N . As shown in Fig. 6, for $l_p = 0$ and $r_c = 3$, chains of length $N = 1,500$ ($1/N = 6.7 \times 10^{-4}$) are already collapsed at $T^* = 60$, whereas the shorter chains are not. This observation suggests that the collapse transition temperature depends on the chain length. As the chain length increases, the transition temperature is expected to approach the θ -point for flexible chains in the thermodynamic limit ($N \rightarrow \infty$).

The chain length also affects the sharpness of the transi-

sition, making it sharper for longer chains, as is illustrated in Fig. 7a and 7b. Comparing the results for $l_p = 3$ and $r_c = 1$ (Fig. 7a) with those for $l_p = 0$ and $r_c = 3$ (Fig. 7b), we find that for flexible chains with longer-range attraction ($l_p = 0, r_c = 3$), the slope does not increase significantly but remains relatively small. Indeed, the curves in Fig. 7b seem to converge for large N to a curve of finite slope. This suggests that for $l_p < r_c$, the transition may not become truly sharp even in the $N \rightarrow \infty$ limit.

To quantify this behavior, we fit the $\langle R_g^2 \rangle / N$ versus T^* data using a sigmoid-like function [see Eq. (8)]. The solid lines in Fig. 7a and 7b show the fitted curves. From these fits, we find that the maximum slope of each fitted curve decreases with $1/N$, as expected (Fig. 7c and 7d). The value for $l_p = 3, r_c = 1$ is approximately 100 times larger than that for $l_p = 0, r_c = 3$, and it increases much more rapidly with chain length.

Thus, both the sharpness and the temperature of the collapse transition vary systematically with chain length, although this dependence is weaker than the influence of l_p and r_c .

IV. CONCLUSIONS

In this study, we have investigated the single-chain collapse of polymer chains using Monte Carlo simulations based on the Pruned-Enriched Rosenbluth Method (PERM). We have analyzed the influence of two key parameters: the persistence length, l_p , associated with the intrinsic stiffness of the polymer chain, and r_c , determining the range of monomer-monomer attraction. The interplay of these two parameters is subtle, affecting the location of the transition temperature and its sharpness. Figure 8 summarizes our main findings in the l_p - r_c plane, illustrating how the competition between chain stiffness and attraction range determines both the sharpness of the collapse and whether stiffness promotes or suppresses

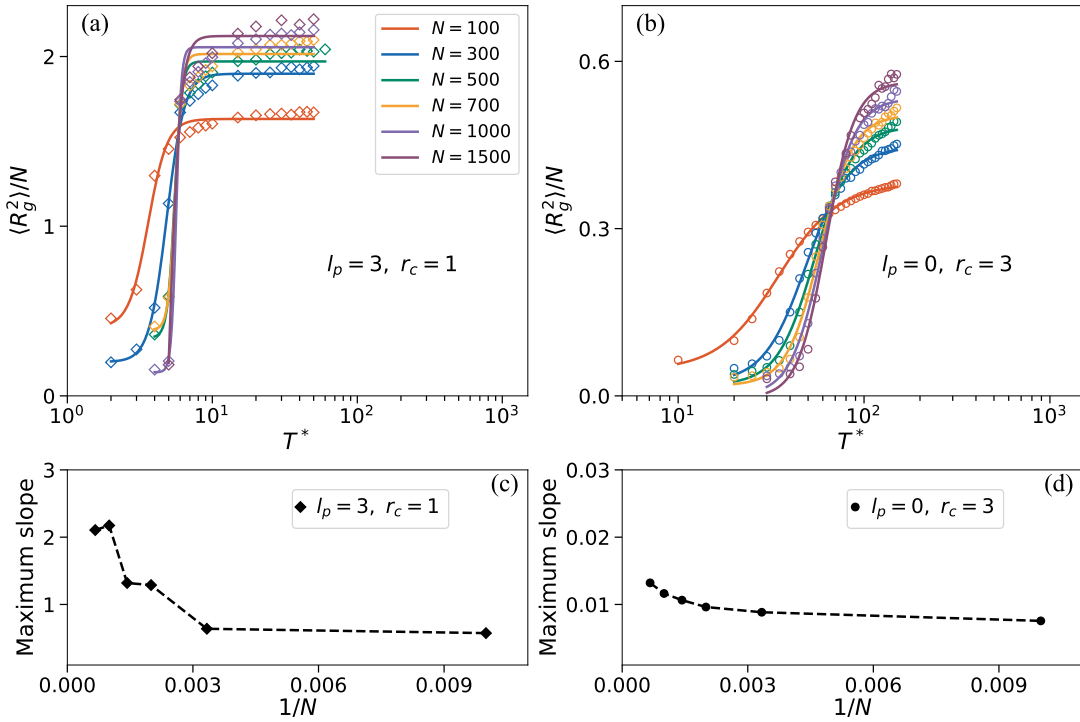


FIG. 7. Temperature dependence of $\langle R_g^2 \rangle / N$ for chain lengths $N = 100, 300, 500, 700, 1,000$ and 1,500. Symbols show simulation data and solid lines are fits to a sigmoid-like function [Eq. (8)]. (a) $l_p = 3, r_c = 1$. (b) $l_p = 0, r_c = 3$. (c) and (d) Maximum slope of the fitted curves as a function of $1/N$. The vertical scale in (d) is two orders of magnitude smaller than in (c). Lines in (c) and (d) are guides to the eye. Diamonds in (a) and (c) correspond to $l_p = 3, r_c = 1$, and circles in (b) and (d) to $l_p = 0, r_c = 3$.

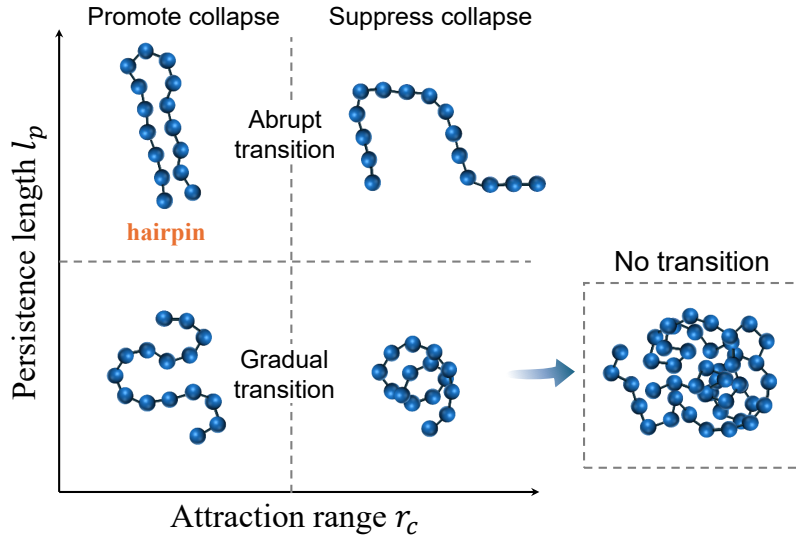


FIG. 8. A schematic illustration of the collapse behavior of a single polymer chain, summarizing the roles of the persistence length l_p and the attraction range r_c .

it.

The Figure shows that increasing the persistence length leads to a sharper collapse transition, whereas expanding the attraction range results in a more gradual collapse. Overall, our results indicate that the sharpness of the collapse transition depends on the competition be-

tween stiffness and interaction range. When $l_p \gtrsim r_c$, stiff chains undergo a sharp and well-defined collapse transition. By contrast, when $l_p \lesssim r_c$, the critical collapse transition is effectively removed, turning into gradual compaction over a finite temperature range. Figure 7 further suggests that this rounding persists upon increasing the

chain length. In cases where the attraction is induced by condensing molecules, this removal of criticality is supported by a scaling argument (see Appendix).

We have examined the dependence of the transition temperature T_θ on chain stiffness. We have found that stiffness may either increase T_θ or decrease it, depending on the attraction range r_c . For small r_c , increasing stiffness promotes collapse and raises T_θ , whereas for large r_c , it suppresses collapse and lowers T_θ . These results (see Fig. 4) provide important insight into the relative role of polymer stiffness and monomer interactions in relation to the collapse transition. This new insight may resolve previous conflicting results concerning the effect of stiffness on the transition temperature.

The polymer chain length N plays a secondary yet systematic role. Longer chains exhibit a sharper transition and slightly shifted transition temperature. However, this effect is significantly weaker than that of l_p and r_c . This suggests that, while stiffness and interaction range dominate the collapse behavior, finite-size effects must be considered when interpreting simulation or experimental data.

Our findings contribute to a more systematic understanding of the polymer phase behavior and may have valuable implications for designing responsive polymeric materials, biomolecular folding, and nanotechnology applications [46–48]. The main conclusion is that a sharp, sensitively controlled collapse (e.g., as in DNA condensation [39]) requires chain stiffness, the more specific criterion being $l_p \gtrsim r_c$. Future research can incorporate solvent effects, adding condensing agents such as multivalent ions, as in the experiments of Knobler, Gelbart, and co-workers [39], or surfactants, and exploring more complex architectures beyond linear polymer chains.

ACKNOWLEDGMENTS

We thank A. Giacometti, H. Orland, and R. Zandi for useful discussions. This work was partly supported by the Israel Science Foundation (ISF) under Grants No. and 226/24 and 1611/24.

Appendix: Scaling argument

We present a heuristic scaling argument for the competing effects of the range of attraction, induced by condensing agents, and the persistence length, on the collapse transition [40]. The analysis is valid in the limit $b \ll l_p, r_c \ll Nb$. Hence, it cannot be directly related to the numerical results presented in the main text. The purpose of the scaling argument is to rationalize the trends we observed in the numerical simulations in a different context. Specifically, we explore the conditions under which an ordinary coil-to-globule transition, occurring at a critical temperature, can be turned by condensing agents into a gradual contraction occurring over a finite temperature range in the thermodynamic limit, $N \rightarrow \infty$.

We express the attraction between any two monomers as

$$u_{\text{att}}(r) = -Af(r/r_c), \quad (\text{A.1})$$

where r is the distance between the monomers in 3D space, A is the attraction strength, assumed to be small compared to the thermal energy $k_B T$, r_c is the attraction range, and $f(r/r_c)$ is a function that decays fast to zero for $r > r_c$. In various scenarios, such as the one considered in Ref. 39, the attraction between monomers does not come from a direct potential but is induced by condensing agents. In such a case A and r_c would not be constant parameters but depend on external conditions, such as the agent concentration. Consequently, in our scaling argument, we treat A and r_c as parameters that can be tuned by the condensing agents.

The attraction reduces the excluded-volume parameter of the chain, $v(T) = v_0 - \delta v(T)$, where v_0 is the excluded-volume parameter in the absence of the attraction, and

$$\begin{aligned} \delta v(T) &= - \int d^3r \left[1 - e^{-\beta u_{\text{att}}(r)} \right] \simeq -\beta \int d^3r u_{\text{att}}(r) \\ &\sim \beta A r_c^3, \end{aligned} \quad (\text{A.2})$$

recalling that $\beta = 1/k_B T$.

When the overall monomer-monomer interaction (consisting of self-avoidance and attraction) is repulsive ($v(T) > 0$), the chain is swollen, whereas when it is attractive ($v(T) < 0$), the chain is collapsed [49]. In the usual situation, where the competing repulsive and attractive interactions have similar (short) ranges, the collapse transition occurs at the sharply defined temperature T_θ for which $v(T_\theta) = 0$ [49].

In a different scenario of gradual contraction, the collapse does not involve all the monomers. We show that the dominance of different interactions on different length scales can bring this about. If the attraction is weak but long-ranged, it will dominate over large distances, while at smaller distances, the repulsive self-avoidance will be the dominant interaction. In such a scenario, the chain can be envisioned as divided into subunits, or ‘blobs’ (a

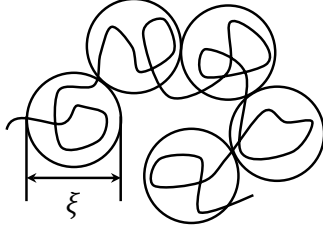


FIG. 9. A schematic illustration of a chain of blobs with blob size ξ .

useful concept introduced by de Gennes and often used in polymer physics [49]).

Imagine that the chain is divided into blobs of spatial size ξ , each containing g monomers, as illustrated schematically in Fig. 9. The behavior of the rescaled ‘chain of blobs’, in which each blob is an effective monomer, is determined by an *effective interaction* $U_{\text{eff}}(r)$ acting between two blobs. This consists of strong inter-blob repulsion at distances smaller than ξ , and attraction at distances larger than ξ due to the integrated attractive interaction of g^2 monomer pairs in the two blobs,

$$U_{\text{eff}}(r) = \begin{cases} \infty, & r < \xi \\ g^2 u_{\text{att}}(r), & r > \xi. \end{cases} \quad (\text{A.3})$$

This effective interaction implies that the rescaled chain of blobs is characterized by an effective excluded-volume parameter, V_{eff}

$$V_{\text{eff}}(T) = \int d^3r \left[1 - e^{-\beta U_{\text{eff}}(r)} \right]. \quad (\text{A.4})$$

Although we have assumed weak monomer-monomer attraction, $A \ll k_B T$ [Eq. (A.1)], the effective attraction between blobs, proportional to $g^2 A$, is not necessarily smaller than $k_B T$. This necessitates the accurate expression for the excluded-volume parameter, Eq. (A.4).

When the chain is in the temperature range of such gradual contraction, the rescaled chain of blobs is in the critical regime. As T is changed within this range, the blob parameters ξ and g adapt to keep the rescaled chain at its collapse transition. Thus, the balance between the competing interactions is such that the rescaled excluded-volume parameter vanishes, $V_{\text{eff}}(T) = 0$. Substituting the expressions for $U_{\text{eff}}(r)$ [Eq. (A.3)] and $u_{\text{att}}(r)$ [Eq. (A.1)] in Eq. (A.4), we can rewrite the condition $V_{\text{eff}} = 0$ as

$$\int_1^\infty \rho^2 d\rho \left[\exp(\beta g^2 A f((\xi/r_c)\rho)) - 1 \right] = \text{const.} \quad (\text{A.5})$$

where $\rho = r/\xi$, and the constant on the right-hand side is of order unity.

The ability of the chain to adjust its subdivision into blobs requires that Eq. (A.5) be satisfied for any temperature within the gradual-contraction range. This can be

achieved only if $\beta g^2 A$ as well as ξ/r_c remain constant.

$$\xi \sim r_c, \quad g \sim (\beta A)^{-1/2}. \quad (\text{A.6})$$

Since we have assumed $\beta A \ll 1$, we get $g \gg 1$, consistently with the blob picture.

At the same time, the size and number of monomers in a blob, ξ and g , are geometrically related. For $g \gg 1$, they satisfy a scaling relation,

$$\xi \sim b g^\nu, \quad (\text{A.7})$$

where ν is the chain Flory exponent on the blob scale. Using Eqs. (A.6) and (A.7) in Eq. (A.2), we obtain

$$g \sim (\delta v/b^3)^{1/(3\nu-2)}, \quad \xi \sim (\delta v/b^3)^{\nu/(3\nu-2)}. \quad (\text{A.8})$$

We now impose a condition of self-consistency on the scenario of gradual contraction through subdivision. The contraction of the chain is caused by a decrease of its excluded-volume parameter, $v = v_0 - \delta v$, *i.e.*, an increase in δv . As the chain contracts, the number of monomers in a blob, g , must decrease. This process stops when $g \sim 1$, resulting in a fully collapsed chain. According to Eq. (A.8), g would decrease with increasing δv only if

$$\nu < 2/3. \quad (\text{A.9})$$

We recall that the value of ν is the one applicable within a blob, *i.e.*, corresponding to the chain without the added attraction. If the chain has a persistence length l_p which is larger than the blob, then within a blob the chain is rod-like, $\nu = 1$, and the self-consistency condition is not fulfilled. If, however, l_p is smaller than the blob, the chain is swollen, $\nu \geq 1/2$, and gradual contraction is self-consistent.

The blob size ξ controls the local chain statistics in the scaling argument, but along the contraction, according to Eq. (A.6), the blob size is set by the induced attraction range r_c . Thus, ξ and r_c are of the same order, and the criterion for sharp versus gradual collapse reduces to comparing l_p with r_c .

$$\begin{aligned} l_p &\gtrsim r_c : && \text{sharp transition} \\ l_p &\lesssim r_c : && \text{gradual contraction.} \end{aligned} \quad (\text{A.10})$$

The scaling argument relies on a mechanism in which the strength and range of the attraction can change (*e.g.*, with temperature or concentration of the condensing agents). While this mechanism is not realized in our simulations, where the attraction is fixed and strictly vanishes beyond r_c , the purpose of this analysis is to demonstrate a concrete mechanism by which an increased range of monomer-monomer attraction is related to the rounding of the critical collapse transition. This relation is qualitatively in line with our numerical observation, indicating that the comparison between l_p and r_c controls the sharpness of the transition.

REFERENCES

- [1] Grosberg, A. Y.; Khokhlov, A. R. *Statistical Physics of Macromolecules*; AIP Press, New York, **1994**.
- [2] Kita, R.; Wiegand, S. Soret Coefficient of Poly(N-isopropylacrylamide)/Water in the Vicinity of Coil-Globule Transition Temperature. *Macromolecules* **2005**, *38*, 4554-4556.
- [3] Frerix, A.; Schonewald, M.; Geilenkirchen, P.; Müller, M.; Kula, M. R.; Hubbuch, J. Exploitation of the Coil-Globule Plasmid DNA Transition Induced by Small Changes in Temperature, pH, Salt, and Poly(ethylene glycol) Compositions for Directed Partitioning in Aqueous Two-Phase Systems. *Langmuir* **2006**, *22*, 4282-4290.
- [4] Tanaka, F.; Koga, T.; Kojima, H.; Winnik, F. M. Temperature- and Tension-Induced Coil-Globule Transition of Poly(N-isopropylacrylamide) Chains in Water and Mixed Solvent of Water/Methanol. *Macromolecules* **2009**, *42*, 1321-1330.
- [5] Nakata, M. Coil-Globule Transition of Poly(methyl methacrylate) in a Mixed Solvent. *Phys. Rev. E* **1995**, *51*, 5770.
- [6] Sherman, E.; Haran, G. Coil-Globule Transition in the Denatured State of a Small Protein. *Proc. Natl. Acad. Sci. U.S.A.* **2006**, *103*, 11539-11543.
- [7] Xu, J.; Zhu, Z.; Luo, S.; Wu, C.; Liu, S. First Observation of Two-Stage Collapsing Kinetics of a Single Synthetic Polymer Chain. *Phys. Rev. Lett.* **2006**, *96*, 027802.
- [8] Stockmayer, W. H. Problems of the Statistical Thermodynamics of Dilute Polymer Solutions. *Makromol. Chem.* **1960**, *35*, 54-74.
- [9] Nishio, I.; Sun, S. T.; Swislow, G.; Tanaka, T. First Observation of the Coil-Globule Transition in a Single Polymer Chain. *Nature* **1979**, *281*, 208-209.
- [10] Swislow, G.; Sun, S. T.; Nishio, I.; Tanaka, T. Coil-Globule Phase Transition in a Single Polystyrene Chain in Cyclohexane. *Phys. Rev. Lett.* **1980**, *44*, 796.
- [11] Lifshitz, I. M. Some Problems of the Statistical Theory of Biopolymers. *Zh. Eksp. Teor. Fiz.* **1968**, *55*, 2408-2422. (Engl. Transl.: Sov. Phys. JETP **1969**, *28*, 1280-1286).
- [12] Lifshitz, I. M.; Grosberg, A. Y.; Khokhlov, A. R. Some Problems of the Statistical Physics of Polymer Chains with Volume Interaction. *Rev. Mod. Phys.* **1978**, *50*, 683-713.
- [13] Grosberg, A. Y.; Kuznetsov, D. V. Quantitative Theory of the Globule-to-Coil Transition. 1. Link Density Distribution in a Globule and Its Radius of Gyration. *Macromolecules* **1992**, *25*, 1970-1979.
- [14] Grosberg, A. Y.; Kuznetsov, D. V. Quantitative Theory of the Globule-to-Coil Transition. 4. Comparison of Theoretical Results with Experimental Data. *Macromolecules* **1992**, *25*, 1996-2003.
- [15] Wu, C.; Wang, X. Globule-to-Coil Transition of a Single Homopolymer Chain in Solution. *Phys. Rev. Lett.* **1998**, *80*, 4092-4094.
- [16] Wu, C.; Zhou, S. First Observation of the Molten Globule State of a Single Homopolymer Chain. *Phys. Rev. Lett.* **1996**, *77*, 3053.
- [17] Baysal, B. M.; Kayaman, N. Coil-Globule Transition of Poly(methyl methacrylate) by Intrinsic Viscosity. *J. Chem. Phys.* **1998**, *109*, 8701.
- [18] Ye, X.; Lu, Y.; Shen, L.; Ding, Y.; Liu, S.; Zhang, G.; Wu, C. How Many Stages Are in the Coil-to-Globule Transition of Linear Homopolymer Chains in a Dilute Solution? *Macromolecules* **2007**, *40*, 4750.
- [19] Chakraborty, I.; Mukherjee, K.; De, P.; Bhattacharyya, R. Monitoring Coil-Globule Transitions of Thermoresponsive Polymers by Using NMR Solvent Relaxation. *J. Phys. Chem. B* **2018**, *122*, 6094.
- [20] Bustamante, C.; Marko, J. F.; Siggia, E. D.; Smith, S. Entropic Elasticity of λ -Phage DNA. *Science* **1994**, *265*, 1599-1600.
- [21] Gerrits, L.; Hammink, R.; Kouwer, P. H. J. Semiflexible Polymer Scaffolds: An Overview of Conjugation Strategies. *Polym. Chem.* **2021**, *12*, 1362-1392.
- [22] Skrbic, T.; Banavar, J. R.; Giacometti, A. Chain Stiffness Bridges Conventional Polymer and Biomolecular Phases. *J. Chem. Phys.* **2019**, *151*, 174901.
- [23] Arcangeli, T.; Skrbic, T.; Azote, S.; Marcato, D.; Rosa, A.; Banavar, J. R.; Piazza, R.; Maritan, A.; Giacometti, A. Phase Behavior and Self-Assembly of Semiflexible Polymers in Poor-Solvent Solutions. *Macromolecules* **2024**, *57*, 8940-8955.
- [24] Leforestier, A.; Livolant, F. Structure of Toroidal DNA Collapsed Inside the Phage Capsid. *Proc. Natl. Acad. Sci. U.S.A.* **2009**, *106*, 9157-9162.
- [25] Leforestier, A.; Siber, A.; Livolant, F.; Podgornik, R. Protein-DNA Interactions Determine the Shapes of DNA Toroids Condensed in Virus Capsids. *Biophys. J.* **2011**, *100*, 2209-2216.
- [26] Seaton, D. T.; Schnabel, S.; Landau, D. P.; Bachmann, M. From Flexible to Stiff: Systematic Analysis of Structural Phases for Single Semiflexible Polymers. *Phys. Rev. Lett.* **2013**, *110*, 028103.
- [27] Marenz, M.; Janke, W. Knots as a Topological Order Parameter for Semiflexible Polymers. *Phys. Rev. Lett.* **2016**, *116*, 128301.
- [28] Majumder, S.; Marenz, M.; Paul, S.; Janke, W. Knots Are Generic Stable Phases in Semiflexible Polymers. *Macromolecules* **2021**, *54*, 5321-5334.
- [29] Yang, D.; Wang, Q. Unified View on the Mean-Field Order of Coil-Globule Transition. *ACS Macro Lett.* **2013**, *2*, 952-954.
- [30] Wang, Z. G. 50th Anniversary Perspective: Polymer Conformation – A Pedagogical Review. *Macromolecules* **2017**, *50*, 9073-9114.
- [31] Post, C. B.; Zimm, B. H. Internal Condensation of a Single DNA Molecule. *Biopolymers* **1979**, *18*, 1487-1501.
- [32] Rampf, F.; Binder, K.; Paul, W. The Single Polymer Chain Phase Diagram: New Insights from a New Simulation Method. *J. Polym. Sci., Part B: Polym. Phys.* **2006**, *44*, 2542-2555.
- [33] Noguchi, H.; Yoshikawa, K. First-Order Phase Transition in a Stiff Polymer Chain. *Chem. Phys. Lett.* **1997**, *278*, 184-188.
- [34] Doniach, S.; Garel, T.; Orland, H. Phase Diagram of a Semiflexible Polymer Chain in a θ Solvent: Application to Protein Folding. *J. Chem. Phys.* **1996**, *105*, 1601.
- [35] Bastolla, U.; Grassberger, P. Phase Transitions of Single Semistiff Polymer Chains. *J. Stat. Phys.* **1997**, *89*, 1061-1078.

- [36] Binder, K.; Paul, W.; Strauch, T.; Rampf, F.; Ivanov, V.; Luettmer-Strathmann, J. Phase Transitions of Single Polymer Chains and of Polymer Solutions: Insights from Monte Carlo Simulations. *J. Phys.: Condens. Matter* **2008**, *20*, 494215.
- [37] Taylor, M. P.; Paul, W.; Binder, K. Phase Transitions of a Single Polymer Chain: A Wang-Landau Simulation Study. *J. Chem. Phys.* **2009**, *131*, 114907.
- [38] Taylor, M. P.; Paul, W.; Binder, K. Applications of the Wang-Landau Algorithm to Phase Transitions of a Single Polymer Chain. *Polymer Sci. Ser. C* **2013**, *55*, 23-38.
- [39] Duran-Meza, A. L.; Oster, L.; Sportsman, R.; Phillips, M.; Knobler, C. M.; Gelbart, W. M. Long ssRNA Undergoes Continuous Compaction in the Presence of Polyvalent Cations. *Biophys. J.* **2023**, *122*, 3469-3475.
- [40] Diamant, H.; Andelman, D. General Criterion for Controllable Conformational Transitions of Single- and Double-Stranded DNA. Unpublished, **2001**. Preprint available at <https://doi.org/10.48550/arXiv.cond-mat/0109253>.
- [41] Grassberger, P. Pruned-Enriched Rosenbluth Method: Simulations of θ Polymers of Chain Length up to 1 000 000. *Phys. Rev. E* **1997**, *56*, 3682.
- [42] Rosenbluth, M. N.; Rosenbluth, A. W. Monte Carlo Calculation of the Average Extension of Molecular Chains. *J. Chem. Phys.* **1955**, *23*, 356.
- [43] Wall, F. T.; Erpenbeck, J. J. New Method for the Statistical Computation of Polymer Dimensions. *J. Chem. Phys.* **1959**, *30*, 634.
- [44] Hsu, H. P.; Grassberger, P. A Review of Monte Carlo Simulations of Polymers with PERM. *J. Stat. Phys.* **2011**, *144*, 597-637.
- [45] Golestanian, R.; Kardar, M.; Liverpool, T. B. Collapse of Stiff Polyelectrolytes due to Counterion Fluctuations. *Phys. Rev. Lett.* **1999**, *82*, 4456.
- [46] Shepherd, J.; Sarker, P.; Swindells, K.; Douglas, I.; MacNeil, S.; Swanson, L.; Rimmer, S. Binding Bacteria to Highly Branched Poly(N-Isopropyl Acrylamide) Modified with Vancomycin Induces the Coil-to-Globule Transition. *J. Am. Chem. Soc.* **2010**, *132*, 1736-1737.
- [47] Patel, A.; Malinovska, L.; Saha, S.; Wang, J.; Alberti, S.; Krishnan, Y.; Hyman, A. A. ATP as a Biological Hydrotrope. *Science* **2017**, *356*, 753-756.
- [48] Rumyantsev, A. M.; Gavrilov, A. A.; Johner, A. Complete Diagram of Conformational Regimes for Polyampholytic Disordered Proteins. *Macromolecules* **2024**, *57*, 5533-5544.
- [49] de Gennes, P.-G. *Scaling Concepts in Polymer Physics*; Cornell University, Ithaca, **1979**.

for Table of Contents use only
Collapse of a single polymer chain:
Effects of chain stiffness and attraction range

